JOHN R. SCHOTT
Calspan Corporation
Buffalo, NY 14225

Temperature Measurement of Cooling Water Discharged from Power Plants

A technique for calibrating a thermal infrared scanner was successfully tested.

ABSTRACT: *In an effort to resolve technical, operational, and cost problems associated with the existing approaches for measurement of water surface temperature, a program was initiated to develop and test a wholly airborne calibration of a thermal scanner system as an alternative. This technique involved development of a model relating the signal at the sensor to the surface temperature and the atmospheric effects contributing to the signal at the sensor.*

Procedures were developed for collection and analysis of the thermal imagery such that the terms in this model could be calculated. Once these terms, including atmospheric transmission, sky radiation, and reflectance of the water, have been determined, the water surface temperature can be calculated. In an effort to evaluate this technique, a series of "blindfold" tests were made. In these tests, an airplane flew over a boat located at different positions in the water at different times and on different days. The aircraft values were then compared to the boat values, which had been withheld until the aerial determinations were made. Results of this test indicate that, on the average, the aerial measurements fell within 0.70°F of the boat temperatures (standard deviation ±0.59°F for 63 points). On the basis of these results, this wholly airborne approach, called the "angular calibration technique," is considered operational for airborne measurement of water surface temperatures.

INTRODUCTION AND SUMMARY

THE GROWING NUMBER and size of power facilities has stimulated the interest of scientists, legislators, and the public in the effects such stations have on aquatic environments. The impact of thermal discharges on aquatic ecology and the effects on aquatic organisms that are drawn through cooling systems are of particular concern. In order to ensure proper protection and management of the environment as well as continued generation of required power, procedures must be developed to accurately assess environmental effects in a timely and cost-effective manner. In monitoring the cooling water discharged into a water body, the temperature value and spatial extent of the thermal plume are the parameters of interest. These thermal plumes can, in some instances, extend more than a mile from the discharge point and include temperature increases in excess of 15°F.

Airborne thermal infrared imaging systems have been used to study some of these problems.[1-3] These systems generate an image (similar to a photograph) of the heat energy radiated by water surfaces. For example, the brighter the water appears on the image, the higher the temperature of the water is. The advantage of this approach is that the thermal scanner can image the entire

PHOTOGRAMMETRIC ENGINEERING AND REMOTE SENSING,
Vol. 45, No. 6, June 1979, pp. 753-761.

surface area of a discharge plume in minutes. In this manner, all the internal detail as well as the shape and spatial extent can be easily determined. The disadvantage of this approach is that a boat is required to provide data needed to convert brightness levels on the image to temperature values.

In an effort to resolve technical, operational, and cost problems associated with the existing approaches, a program was initiated to develop and test wholly airborne calibration of a thermal scanner system so that precise thermal maps could be generated without requiring data from boats. This technique involved development of a model relating the signal at the sensor to the surface temperature and the atmospheric effects contributing to the signal at the sensor.

Procedures were developed for collection and analysis of the thermal imagery such that the terms in this model could be calculated. Data collection procedures included flying the aircraft at different altitudes over the same point in the water and flying parallel flight lines so that data from points in the water could be viewed at different look angles. These procedures add a minimal amount of time to data collection and provide sufficient data so that an analysis of the terms relating water temperature to the signal actually reaching the sensor can be calculated. Once these terms, including atmospheric transmission, sky radiation, and reflectance of the water, have been determined, the water surface temperature can be calculated.

In an effort to evaluate this technique, a series of "blindfold" tests was made.[4] In these tests an airplane flew over a boat located at different positions in the water at different times and on different days. The aircraft values were then compared to the boat values, which had been withheld until the aerial determinations were made.[5] Results of this test indicate that, on the average, the aerial measurements fell within 0.70°F of the boat temperatures (standard deviation ±0.59°F for 63 points). On the basis of these results, this wholly airborne approach, called the "angular calibration technique," is considered operational for airborne measurement of water surface temperatures.

This paper discusses the airborne calibration technique and the experimental test program. For the sake of brevity, the details of the airborne collection system are omitted and the assumption is made that the radiant energy reaching an airborne sensor can be converted to an apparent blackbody temperature equivalent.

Theoretical Approach

Thermal scanners generally detect radiation in the 8-14 μm bandpass. This section will discuss how the radiant energy detected by a sensor at aircraft altitudes (~600 m) is not only a function of temperature but is also functionally dependent on atmospheric and background terms. In addition, the types of measurements required to calculate the values of these additional terms will be defined.

All matter at temperatures above absolute zero radiates electromagnetic energy. The relation between blackbody radiant emittance, W, and temperature, T, in °K is expressed by the Stefan-Boltzmann equation

$$W = \sigma T^4, \tag{1}$$

where σ is the Stefan-Boltzman constant.

The general equation for a blackbody radiator is given by the Planck distribution equation,

$$W_\lambda = 2\pi c^2 h \lambda^{-5} (e^{hc/\lambda kT} - 1)^{-1}, \tag{2}$$

where W_λ is the radiant emittance per unit wavelength interval,

c is the speed of light,
h is Planck's constant,
k is Boltzmann's constant,
T is temperature, and
λ is wavelength.

This equation, derived from quantum physics, is a function of the quantum radiation states within a blackbody cavity.

The Stefan-Boltzmann equation is obtained by integrating the Planck equation over all wavelengths.

The problem in using these equations is finding the dependence of W on temperature over a defined bandpass. The Stefan-Boltzmann equation indicates that radiant emittance integrated over all wavelengths varies as T^4, i.e.,

$$\int_0^\infty W_\lambda \, d\lambda = W = \sigma T^4. \tag{3}$$

To find the functional dependence on temperature in a finite bandpass, it is necessary to use a series expansion solution to the normalized integral of radiant emittance. This yields the fraction of energy less than a given wavelength, D, given by

$$D = \frac{\int_0^\lambda W_\lambda \, d\lambda}{\int_0^\infty W_\lambda \, d\lambda}. \tag{4}$$

These D values are tabulated in standard blackbody tables for ranges of T, λ, or λT combinations.[6] By finding the difference in D for two wavelengths, a relation can be developed between temperature and radiant emittance in a bandpass expressed as a fraction of the total radiant emittance.

If D is the fraction of the total energy emitted by a blackbody between the wavelength 0 and λ, then $D_1 - D_2$ is the fraction of emitted energy between λ_1 and λ_2. Since σT^4 is the total energy for a given temperature, then $W = (D_1 - D_2)\,\sigma T^4$ is the radiant energy emitted for a given bandpass. Values of W and T over the range of interest can be stored in data files on a computer. T can be calculated from the stored W values.

We can therefore express the radiant energy from a blackbody over the 8-14 μm bandpass ($W_{\Delta\lambda}$) as

$$W_{\Delta\lambda} = W_T = \int_8^{14} 2\pi c^2 h \lambda^{-5} (e^{hc/\lambda kT} - 1)^{-1}\, d\lambda. \tag{5}$$

This expression, however, is only true for a blackbody. A blackbody is a perfect radiator and absorber; therefore, all the incident energy is absorbed and reradiated. In practice, the bodies we will be concerned with will be gray bodies, which are not perfect absorbers or radiators in the 8-14 μm bandpass and thus have emissivities less than unity.

Emissivity (ϵ) is the ratio of energy radiated from a source to energy radiated from a blackbody at the same temperature. Thus, for a gray body,

$$W = \epsilon\, W_T. \tag{6}$$

In order to interpret the radiant energy reaching a point at any distance from the source, one must consider atmospheric or path effects; of prime concern is atmospheric transmission over the path lengths of interest. The atmospheric transmission window between 8 and 14 μm is the most useful for earth observation work for a number of reasons. It encompasses the radiant energy peak of 9.5 μm for objects near earth ambient temperature of 300°K. The transmission is quite high over the entire window, and the window is spectrally very broad, permitting integration over a sizable fraction of the total energy radiated.

Primary attenuation in the lower atmosphere is due to absorption by H_2O vapor, CO_2, and OH. These molecules absorb the radiation and reradiate it as a function of temperature, thereby introducing two noise terms into the system.

These terms can be included in the expression we have defined as follows:

$$W = \tau\epsilon W_T + W_A \tag{7}$$

where τ is the atmospheric transmission and W_A is the apparent radiant emittance from the air column between the source and sensor, as well as energy scattered into the sensor. It is important to keep in mind that W_A and τ vary as a function of atmospheric conditions on a given day and also within the air column because of layering effects in the atmosphere.

In addition to the radiant energy from the source itself, a certain amount of energy will be reflected from the ground. This energy comes from both the sun and the sky. Solar reflection effects can be avoided by proper orientation of flight lines. Skylight reflection effects can be expressed as $W_s\,\tau R$ and included in Equation 7, yielding

$$W = \tau\epsilon W_T + W_A + W_s\,\tau R \tag{8}$$

where W_s is the radiant energy from the sky incident on the surface observed, and can be associated with an equivalent sky temperature, T_s. R is the surface reflectance of the water.

Skylight irradiance comes from scattered solar radiation, radiation emitted from components of the atmosphere (especially the ozone layer and H_2O vapor), and energy from the Earth reflected by the atmosphere. All these effects combine to give the sky an apparent radiometric temperature as viewed from the ground. For our purposes, this is the blackbody temperature equivalent, T_s, associated with the amount of energy incident on the source over the bandpass of interest. T_s can vary considerably with sky conditions from about 300°K for heavy overcast to well below 250°K for clear sky conditions.

In evaluating the range of values for the reflectance terms, we recognize that reflection is dependent on look angle. In addition, we have mentioned that W_A and τ are dependent on the length and composition of the atmospheric path between the source and observation point. To recognize this dependence in Equation 8, the functional dependence on θ and h will be added to designate angular and height dependence, respectively,

where h is the height of sensor above terrain,
θ is look angle measured from the vertical, and

$$W(h, \theta) = \tau(h,\theta)\, \epsilon(\theta)\, W_T + W_A(h,\theta) + \tau(h,\theta)\, W_s\, R(\theta). \quad (9)$$

Limiting our discussion for the moment to vertical viewing, ($\theta = 0$), results in

$$W(h) = \tau(h)\epsilon\, W_T + \tau(h)\, W_s\, R + W_A(h). \quad (10)$$

Letting $W(0)$ be the energy from the ground as it would be measured vertically at zero altitude, Equation 10 reduces to

$$W(h) = \tau(h)\, W(0) + W_A(h) \quad (11)$$

where $$W(0) = \epsilon W_T + W_s R. \quad (12)$$

If $W(h)$ and $W(0)$ are known for a set of observed values, then, by least-squares analysis of Equation 11, $\tau(h)$ and $W_A(h)$ can be calculated. $W(h)$ and $W(0)$ represent the radiant energy observed by the sensor at flight altitude and ground level, respectively. In practice, the ground level measure is obtained by extrapolating a plot of altitude-versus-temperature to zero altitude using data collected over the same point at a series of altitudes, where radiant energy is converted to apparent blackbody temperature.

If we once again consider the angular viewing effects, Equation 11 becomes

$$W(h,\theta) = \tau(h,\theta)\, W(0,\theta) + W_A(h,\theta) \quad (13)$$

where

$$W(0,\theta) = \epsilon(\theta)\, W_T + W_s\, R(\theta), \quad (14)$$

$$\tau(h,\theta) = \tau(h,0) \exp(1/\cos\theta), \text{ and} \quad (15)$$

$$W_A(h,\theta) = W_A(h, 0)/\cos\theta. \quad (16)$$

These equations result from the increase in absorption with path length (Equation 15) and the increase in atmospheric radiation with path length (Equation 16). Since the path length increases as $1/\cos\theta$ for slant viewing and the effects on atmospheric emissions should be very nearly linear for small increases in path length through a given medium, Equation 16 is derived. Note that this assumption of linearity is only valid for increase due to slant viewing through a known atmosphere and is not necessarily valid for an overall increase in path length.

If observations were made at the same altitude of a given point through two different look angles, one of which may be taken as vertical for convenience, then Equations 10, 13, and 14 may be combined to yield

$$W(h, 0) = m\, W(h, \theta) - m\tau(h, \theta)\, W_s\, R(\theta) - mW_A(h,\theta) + \tau(h, 0)\, W_s R(0) + W_A(h, 0) \quad (17)$$

where $$m = \frac{\epsilon(0)\, \tau(h, 0)}{\epsilon(\theta)\tau(h,\theta)}. \quad (18)$$

Recognizing this as a straight line in the form,

$$W(h, 0) = mW(h, \theta) + I \quad (19)$$

and solving for W_s in terms of m and I yields

$$W_s = \frac{I + mW_A(h,\theta) - W_A(h, 0)}{\tau(h, 0)\, R(0) - m\tau(h,\theta)\, R(\theta)}. \quad (20)$$

Least-squares analysis of Equation 19, with input data consisting of apparent temperatures (converted to radiant energy) measured along a line viewed vertically and then at a slant angle, will yield from Equation 20 a measure of apparent sky temperature as viewed from the ground.

We have assumed that the apparent temperature of the sky is a constant with respect to angle of observation. In general, this is not the case; rather, the zenith sky appears colder than the sky near the horizon because the atmosphere viewed vertically has fewer radiators. Because of the variability of sky conditions, a functional relationship between sky temperature and view angle is not readily defined nor are the errors introduced by the assumption of a constant sky easily evaluated. In order to minimize potential errors in measured sky temperature, the analysis discussed above can be conducted for a number of look angle combinations, and a simple relationship between T_s and θ can be developed.

Another solution would involve use of a vertical-viewing, upward-looking radiometer on board the aircraft. Measurement of vertical sky temperature at a number of altitudes and extrapolation to the apparent temperature of the nadir sky as viewed from the ground would eliminate one unknown in Equation 17. The equation could then be solved for the sky temperature at look angle θ (i.e., T_s associated with $R(0)$ would be known and T_s associated with $R(\theta)$ would be unknown).

Rewriting Equation 9 as

$$W_T = [W(h,\theta) - \tau(h,\theta)\, W_s\, R(\theta) - W_A(h,\theta)]/\epsilon(\theta)\, \tau(h,\theta), \quad (21)$$

we find

$W(h,\theta)$	is a measured value;
$W_A(h,\theta)$	is obtained from Equation 16 and least-squares analysis of Equation 11;
$\tau(h,\theta)$	is obtained from Equation 15 and least-squares analysis of Equation 11;

W_s is obtained from Equation 20; and

$R(\theta)$ and $\epsilon(\theta)$ are tabulated values for water.

It should therefore be possible to measure the absolute value of surface waters based on the theories developed thus far. The next section contains procedural approaches for collection of necessary input data to solve for the values in Equation 21.

Experimental Design

Our concern at this point is in defining procedures for collecting sufficient input data to permit the use of the theoretical procedures under discussion. Again, we will neglect, for simplicity, signal processing through the sensor and assume that apparent blackbody radiometric temperature can be measured at the sensor location by converting radiant energy to equivalent blackbody temperature.

As shown in Equation 11, the input data necessary to calculate the transmission term τ(h) and the additive target-independent energy from the atmosphere $W_A(h)$ consist of $T_B(h)$ and $T_B(0)$ corresponding to $W(h)$ and $W(0)$. $T_B(h)$ is simply the apparent blackbody temperature measured at altitude h with look angle $\theta = 0$. $T_B(0)$ is the apparent temperature measured at the surface of the water. This value cannot be measured directly but is obtained by a profile technique which involves a simple extrapolation process for data collected at a series of altitudes to a zero altitude case obtained by consecutive flights over the same target.[7] A target consists of an area of uniform temperature either large enough to be directly below the aircraft during the profile or within about 10° from the nadir and distinct enough to be identifiable on the profile images. At angles much larger than 10° the assumption of vertical viewing during the profile no longer holds.

The minimum data input required for Equation 11 is $T_B(h)$ and a corresponding $T_B(0)$ for at least two points at differing temperature. Ideally, these data consist of a set of approximately five data points covering as wide a temperature range as possible. Figure 1 indicates how $T_B(h)$ and $T_B(0)$ could be obtained for a number of different temperatures.

The input data necessary to calculate W_s, the sky radiance term, comes from the solution of Equation 19, requiring $T_B(h, 0)$ and $T_B(h,\theta)$ as inputs. These values are the apparent temperature observed at the same point through two look angles where one look angle is chosen as zero degrees for convenience. (Note also that Equation 11 can be solved directly for W_s, i.e., a one point solution is available). The minimum data required to solve Equation 19 consist of two data sets composed of $T_B(h,0)$ and $T_B(h,\theta)$ for two distinct points. In general, a number of points with a large range in temperature should be used to solve for m and I in Equation 19. This data set can be collected by flying two parallel flight lines and allowing for some sidelap. This procedure is often used to obtain complete target coverage and would add little or no time to most collection efforts. Figure 2 illustrates how these data could be obtained.

A ground-truth program was used to evaluate these radiometric calibration techniques. This effort involved aerial overflights of a boat anchored at a series of positions in the Hudson River, both within and beyond the thermal plumes of various power plants.

With the boat anchored at a given position, readings were made on the upstream (downstream if flow was upstream in the estuary) side of the boat. Measurements consisted of temperatures recorded from a submerged thermistor (nominally at a depth of 6 in.) and from a Barnes PRT-5 radiometer. During each fly-over, approximately ten readings were recorded and averaged to predict the temperature at a point. To insure unbiased data, all surface measurements were made by independent consultants and surface data were withheld until aerial results had been delivered to the New York State Energy Research and Development Authority (NYSERDA). The surface radiometer was calibrated in the field under prevailing atmospheric conditions to ensure that all measurements were absolute surface temperature measurements.

The main survey took place on September 24, 1976 with the boat anchoring at eight positions throughout the day. The aircraft flew over each position four times, permitting 32 data-comparison points for the total survey. Because the boat was covered with aluminum foil, it had a low emissivity and could be located as a "cold" spot on the image. Surface temperatures were predicted using the calibration technique discussed above. Data were also collected at eight positions for five overflights on both July 8 and 9, 1976. However, the July 8 data could not be used because of calibration problems with the surface instrument.

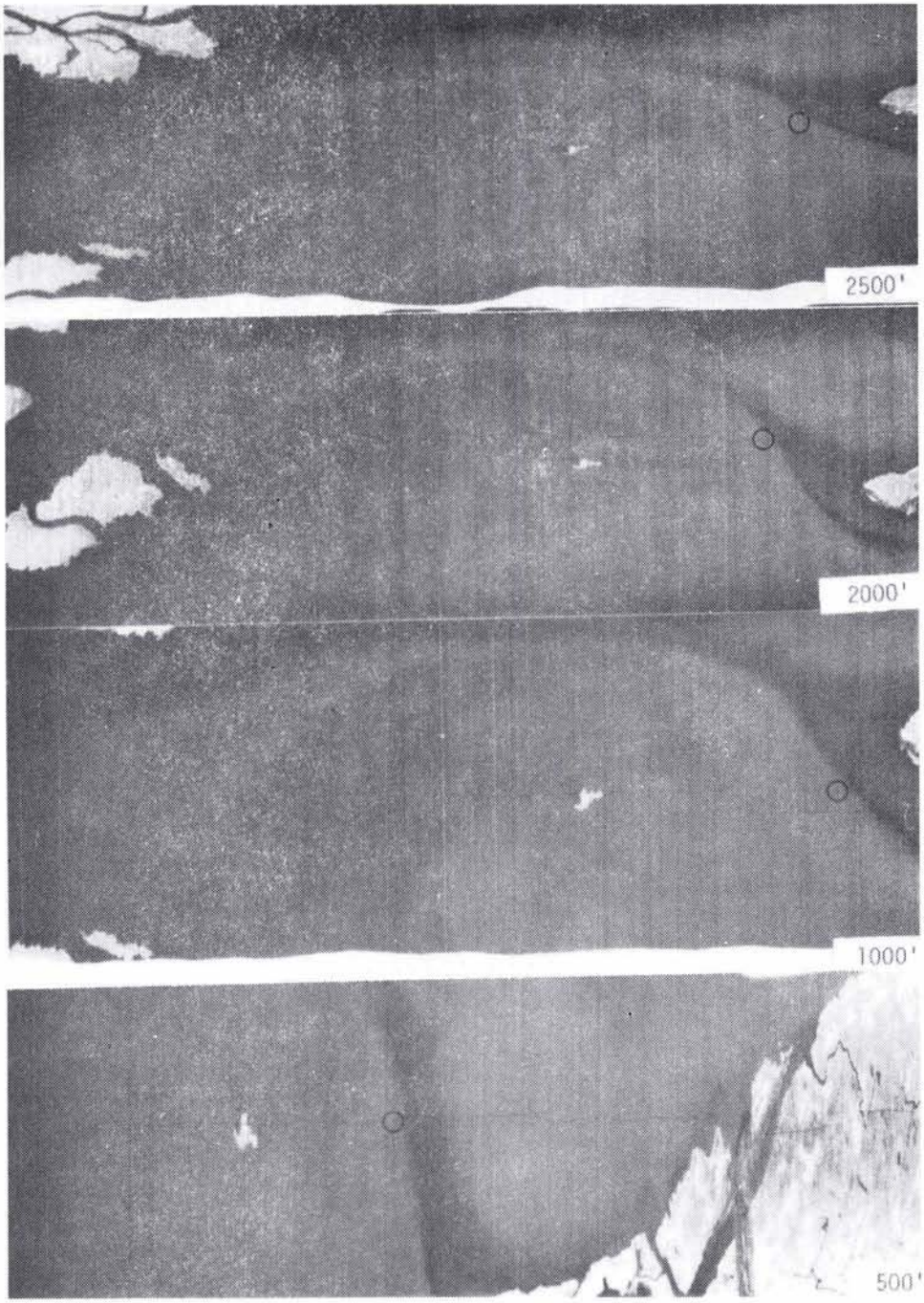

FIG. 1. Thermal images obtained during a profile. Areas of equal temperature where apparent temperature readings could be made are indicated.

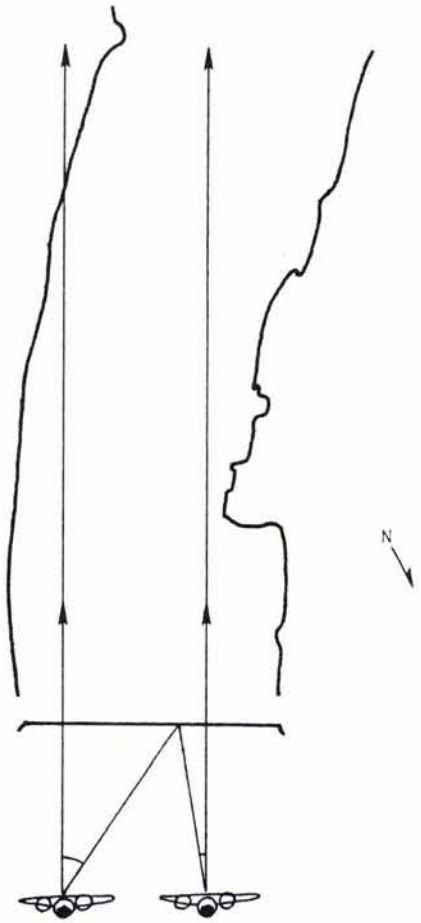

FIG. 2. Example of parallel flight lines over a power station showing the change in look angle for a given ground point.

RESULTS

Table 1 presents the results of the data correlation for September 24. The mean and standard deviations of the absolute value of the difference between the aerial and surface data are presented. Radiometric surface data were used because they are a more accurate measure of the actual surface temperatures than is the submerged thermistor. Comparison of submerged (6 in.) thermistor data and aerial data showed a mean difference of 0.51°F with a standard deviation of ±0.46°F. Also included is a correlation of radiometric temperatures, to which no atmospheric correlations have been applied, with the surface data. Table 2 contains the results of the July 9 survey.

When the July and September data are combined, a mean error of 0.70°F is obtained with a standard deviation of ±0.59°F (Angular Technique). This compares with a mean error of 3.23°F with a standard deviation of ±1.25°F if only internal system calibration is used. Figure 3 illustrates the precision of the calibration technique and the limitations of using only internal scanner calibration. The figure shows the surface radiometer data plotted against the calibrated (⋆) and uncalibrated (□) scanner data. The data, which have been corrected for atmospheric and background effects, show a very close fit within the 1°F error bars. The data using only the internal scanner calibration show sizable errors and are generally less than the actual temperature. Note that this is generally the case but that a temperature higher than the true surface temperature can be detected by airborne systems under certain atmospheric and background conditions.

One shortcoming to the angular technique is a requirement for extra data to permit calibration and some additional data processing. Neither the time nor the cost is appreciable; however, the data must be properly collected. Some improvements in accuracy could be expected if data collection were modified to facilitate analysis using the angular technique. Major improvements cannot be expected because temperatures predicted from the air approach the accuracies obtainable by surface measurements.

CONCLUSIONS AND RECOMMENDATIONS

The data correlation results presented in the previous section indicate that a major advance in airborne radiometric measurement of water surface temperatures has been achieved.[8] Measurement accuracies essen-

TABLE 1. COMPARISON OF SURFACE AND AERIAL DATA FOR 24 SEPTEMBER 1976 (°F)

	Surface Radiometer and Uncorrected Airborne Scanner	Surface Radiometer and Angular Technique
Mean of the absolute value of the temperature difference between boat and aircraft.	4.19	0.55
Standard deviation of ΔT	±1.22	±0.57

TABLE 2. COMPARISON OF SURFACE AND AERIAL DATA FOR JULY 9, 1976 (°F)

	Surface Radiometer and Uncorrected Airborne Scanner	Surface Radiometer and Angular Technique
Mean of the absolute value of the temperature difference between boat and aircraft	2.66	0.80
Standard deviation of ΔT	±1.27	±0.57

tially as good as surface measurements are demonstrated.

The data collection procedures involve only minor variations in standard collection practices requiring approximately 15 additional minutes of flight time. All data processing can be done on a desk-top computer.

The net result of these conclusions is that a fully airborne approach to measure water surface temperatures, with accuracies comparable to those obtained from surface measurements, is an operational possibility. In addition, these results were obtained through use of an outside consultant for acquisition of ground-truth data, thus precluding any bias.

We recommend that future efforts in this area be directed at techniques to generate thermal maps with appropriate corrections at angles away from vertical. The corrections developed using the angular calibration techniques are quite accurate and should be applied in map generation. Current mapping techniques do not apply a correction for variations in apparent temperature at non-vertical look angles; development of these corrective procedures in the map-generation process would allow the full accuracies developed in the angular calibration technique to be carried through to a final map product. In addition, data collected specifically for analysis using this technique should eliminate the need for iterative solutions and should further improve calibration accuracies. While major improvements in water temperature measurements could not be expected because the current results already so closely approach surface measurements, improvements applicable to such problems as a quantitative measurement of heat loss from buildings could be expected. In fact, a major advantage of this technique is that it includes consideration of sufficient variables

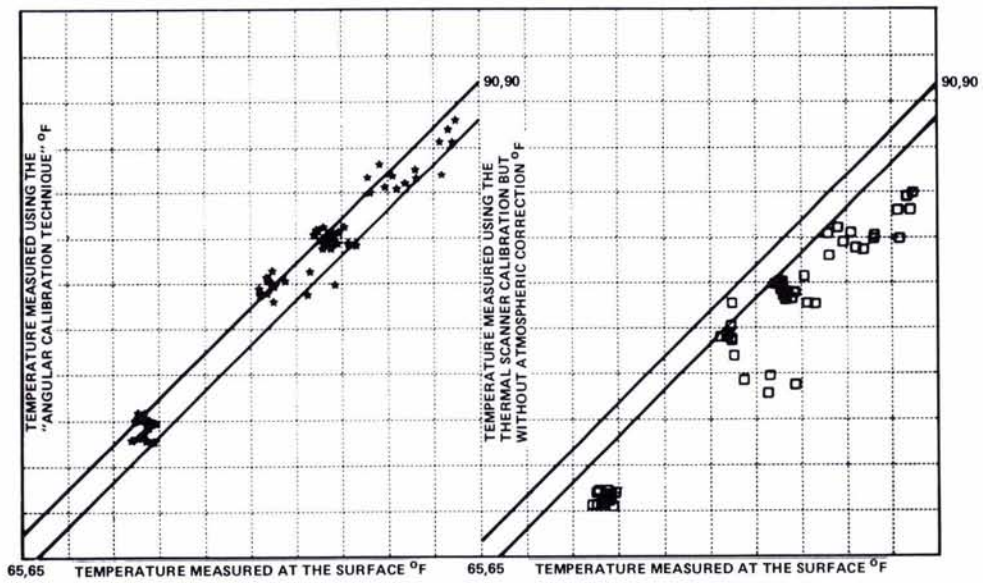

FIG. 3. Comparison of surface and aerial temperature measurements (the lines represent a 1°F error envelope).

to allow surface temperature measurement of any uniform flat surface whose emissitivity is known.

ACKNOWLEDGMENT

The work reported was sponsored by the New York State Energy Research and Development Authority (NYSERDA) under an agreement dated August 23, 1976 with Calspan Corporation.

REFERENCES

1. Bartolucci-Castedo, L. A., *et al., Computer Aided Processing of Remotely Sensed Data for Temperature Mapping of Surface Water from Aircraft Altitudes,* LARS Publication, Purdue University, Indiana, 1973.
2. Haynes, R. B., and J. Whipple, *Problems in Applying Infrared Reconnaissance Technology to Water Temperature Surveillance,* Technical Memorandum No. RADC/IR/TM-71-2, 1971.
3. Scapace, F. L., R. P. Madding, and T. Green III, *Scanning Thermal Plumes,* Ninth International Symposium on Remote Sensing of Environment, April 1974.
4. Schott, J. R., *Thermal Remote Sensing Calibration Techniques,* Calspan Report NA-6019-M-1, NTIS #TB-269-471, 1977.
5. *Report of Infrared Water Temperature Measurements Made September 24, 1976 of the Hudson River,* Wormser Scientific Co. Report, Stamford, Connecticut.
6. Pivovonsky, M., and M. R. Nagel, *Tables of Black Body Radiation Functions,* The MacMillan Company, New York 1961.
7. Schott, J. R., and R. H. Tourin, "A Completely Airborne Calibration of Aerial Infrared Water Temperature Measurements," Proceedings *ERIM Tenth International Symposium on Remote Sensing of Environment.*
8. Schott, J. R., and T. W. Gallagher, "Profile Technique For Calibration of Infrared Thermal Imaging Systems" U.S. Patent 3,970,848 July 20, 1976.

(Received January 4, 1978; revised and accepted February 28, 1979.)

Call for Papers
Ocean Optics IV

Naval Postgraduate School, Monterey, California
October 23-25, 1979

This three-day seminar on all aspects of Ocean Optics, sponsored by the Society of Photo-Optical Instrumentation Engineers and cosponsored by the U.S. Naval Postgraduate School, will provide both a tutorial introduction for newcomers to the field and an overview of state-of-the-art developments for specialists from government, industry, and universities. The first two days, 23-24 October, will consist of unclassified sessions, with the third day, 25 October, reserved for classified presentations and discussions.

Special emphasis will be placed on optical remote sensing of marine resources and ocean optical properties from satellites. A geographical summary of ocean optical properties and their continuing measurements by in situ and remote techniques is planned. Remote optical mapping of water depth and submerged hazards to navigation will be discussed, and military underwater electro-optical systems will be described. Underwater imagery by photographic and television cameras will be discussed, both in principle and in practice.

Those wishing to present papers please send a brief professional biography and a one-paragraph abstract (200 words maximum) by June 22, 1979 to

SPIE Tech Programs Committee
P.O. Box 10
Bellingham, WA 98225
Phone 206-676-3290